

Chapter 3 Effects of Temperature Fluctuations on CFC-11 Transport from the Atmosphere to the Water Table

3.1 Introduction

Transport of atmospheric gases from the land surface to ground water beneath the water table is impacted by unsaturated-zone flow and transport processes. The effect of these processes on concentrations of dissolved gases in ground water may impact the use of these gases as environmental tracers for ground-water age dating and estimation of saturated-zone transport properties. Much attention has been focused on the behavior of chlorofluorocarbons (CFC's) and other gases in arid regions, where the unsaturated zone is relatively thick. However, less attention has been paid to processes affecting dissolved gas concentrations in humid regions, or in regions where the water table is close to the land surface.

Cook and Solomon (1995) used a simple one-dimensional transport model to characterize transport of CFC-11, -12, and -113, and Krypton-85 (⁸⁵Kr) from the land surface to the water table. When the water table is deep, concentrations of these gases in water at the water table lag behind atmospheric concentrations because of the time required for diffusion in the unsaturated zone (Table 3-1). Cook and Solomon (1995) also examined the impact of temperature, unsaturated-zone moisture content, sorption, and recharge rate on concentrations at the water table. Some of the simplifying assumptions used by Cook and Solomon (1995) include isothermal conditions (constant and uniform temperature) and uniform moisture content throughout the unsaturated zone, with a step change in moisture content at the water table.

In this Chapter, the work of Cook and Solomon (1995) is extended by including the effects of more realistic moisture-content distributions in the unsaturated zone, and by

simulating a seasonal temperature profile. Moisture content varies in the unsaturated zone as a function of both elevation above the water table and recharge rate. Furthermore, layers of fine-grained soil have different moisture retention properties than coarser-grained soil, so material heterogeneities can influence unsaturated-zone transport. Similarly, the seasonal temperature profile caused by the seasonal pattern in land surface temperatures, and the heat-transport properties of the porous media effect dissolved-gas transport. The simulations here include these additional factors, and focus on cases with shallow water-table depths, compared to those of Cook and Solomon (1995); these shallow water-table depths may be more characteristic of humid locations in the northeastern U.S., such as the Mirror Lake NH site. After describing the mathematical and numerical model used to simulate one-dimensional water flow and dissolved gas transport, the effect of depth-varying moisture content and nonisothermal conditions are examined for homogeneous and layered unsaturated zones.

Table 3-1. Simulated air-phase concentrations in 1992 of CFC's and Krypton-85 immediately above the water table (Cook and Solomon, 1995) [apparent lag time, in years, given in parentheses]

Water Table Depth (m)	CFC-11 (pptv)	CFC-12 (pptv)	CFC-113 (pptv)	⁸⁵ Kr (dpm cm ⁻³)
0	292	523	86	59
5	289 (0.4)	519 (0.3)	85 (0.3)	59 (0.1)
10	278 (1.5)	504 (1.0)	79 (1.4)	56 (0.6)
20	237 (5.6)	445 (3.9)	57 (4.4)	48 (2.2)
30	174 (12.4)	356 (8.6)	35 (8.2)	37 (4.6)
40	117 (17.2)	263 (14.1)	20 (12.7)	28 (7.3)

3.2 Governing Equations, Constitutive Relations, and Numerical Solution

3.2.1 Governing Equations and Boundary Conditions

In this section, the governing partial differential equations for flow and transport in the unsaturated zone are presented. The flow equation is a mixed form of the Richards' equation for one-dimensional vertical unsaturated water flow. Under steady water flow conditions, air flow is assumed to be zero. Although transport occurs in both the air and water phases, a single transport equation written in terms of only one concentration can be developed because of the equilibrium assumption for local equilibrium air/water partitioning.

Water Flow

Assuming that water is incompressible, a one-dimensional mass conservation equation for the water can be written:

$$\frac{\partial \theta}{\partial t} = - \frac{\partial q}{\partial z} \quad (3.1)$$

where θ [-] is the moisture content and q [LT^{-1}] is the water flux. It is assumed that the water density is unaffected by pressure, temperature, or solute concentration.

Substitution of Darcy's Law for water flow in porous media into the mass conservation equation (3.1), a mixed-form of Richards' equation can be written (Hillel, 1982):

$$\frac{\partial \theta}{\partial t} = \frac{\partial}{\partial z} \left[K(\theta) \left(\frac{\partial h}{\partial z} - 1 \right) \right] \quad (3.2)$$

where $K(\theta)$ [LT^{-1}] is the unsaturated hydraulic conductivity; and h [L] is the pressure head. The coordinate system is oriented downward so that the gravitational gradient acts in the positive z direction. The constitutive relations between the moisture content and

the pressure head, and between moisture content and unsaturated hydraulic conductivity, are presented in Section 3.2.2. Cases presented here are limited to steady flow, in which case (3.2) becomes a nonlinear ordinary differential equation in the pressure head.

The flow equation boundary conditions are either specified flux or specified pressure head at the top and bottom of the domain. Specified pressure boundary conditions at the domain top and bottom are:

$$h = H_0 \text{ at } z = 0 \quad h = H_L \text{ at } z = L \quad (3.3)$$

Alternatively, the fluxes can be specified:

$$K(\theta) \left(1 - \frac{\partial h}{\partial z} \right) = q_0 \text{ at } z = 0 \quad K(\theta) \left(1 - \frac{\partial h}{\partial z} \right) = q_L \text{ at } z = L \quad (3.4)$$

Mixed boundary conditions can be used such that one boundary is specified pressure and the other is specified flux.

Transport

A one-dimensional transport equation considering advection and dispersion/diffusion in both air and water phases can be written (c.f. Cook and Solomon, 1995):

$$\frac{\partial(\theta c + \theta_a c_a)}{\partial t} = \frac{\partial}{\partial z} D \frac{\partial c}{\partial z} - \frac{\partial(qc)}{\partial z} + \frac{\partial}{\partial z} D_a \frac{\partial c_a}{\partial z} - \frac{\partial(q_a c_a)}{\partial z} \quad (3.5)$$

where c [ML^{-3}] is the volumetric concentration in the water phase; c_a [ML^{-3}] is the volumetric concentration in the air phase; θ_a [-] is the air content; q_a [LT^{-1}] is the volumetric air flux; D [L^2T^{-1}] is the water-phase dispersion coefficient; and D_a [L^2T^{-1}] is the air-phase dispersion coefficient. Assuming that partitioning between the air and water phases occurs quickly, relative to vertical transport processes, the air and water phase concentrations can be assumed to be in thermodynamic equilibrium, as expressed by Henry's Law:

$$c_a = \frac{c}{K_w} \quad (3.6)$$

where the Henry's Law coefficient, K_w [-], is generally a function of temperature, pressure and salinity (Warner and Weiss, 1985). The effects of pressure and salinity on K_w are ignored here, and the temperature dependence is described in Section 3.2.2.

Substitution of (3.6) into (3.5) and rearrangement gives

$$\frac{\partial(\theta + \theta_a/K_w)c}{\partial t} = \frac{\partial}{\partial z} \left[D \frac{\partial c}{\partial z} + D_a \frac{\partial(c/K_w)}{\partial z} \right] - \frac{\partial qc}{\partial z} - \frac{\partial q_a c/K_w}{\partial z} \quad (3.7)$$

The governing transport equation is a linear partial differential equation in the water-phase concentration. However, coefficients in the equation may change in time and space due to water and air flow, and changing temperature. The transport equation could also be formulated in term of the air phase concentration (Cook and Solomon, 1995).

Terms appearing in the transport equation related to the divergence of air and water fluxes can be simplified, for example:

$$\begin{aligned} \frac{\partial \theta c}{\partial t} + \frac{\partial qc}{\partial z} &= c \left(\frac{\partial \theta}{\partial t} + \frac{\partial q}{\partial z} \right) + \theta \frac{\partial c}{\partial t} + q \frac{\partial c}{\partial z} \\ &= \theta \frac{\partial c}{\partial t} + q \frac{\partial c}{\partial z} \end{aligned} \quad (3.8)$$

because the parenthetical term is zero, from eq. (3.1). Using the same simplification for air-phase continuity, (3.3) can be written:

$$\theta \frac{\partial c}{\partial t} + \theta_a \frac{\partial(c/K_w)}{\partial t} = \frac{\partial}{\partial z} \left[D \frac{\partial c}{\partial z} + D_a \frac{\partial(c/K_w)}{\partial z} \right] - q \frac{\partial c}{\partial z} - q_a \frac{\partial(c/K_w)}{\partial z} \quad (3.9)$$

If the spatial and temporal gradients in the Henry's Law coefficient are zero, for example under isothermal conditions, or if the gradients are assumed to be essentially zero, then (3.10) can be written (c.f. Cook and Solomon, 1995):

$$(\theta + \theta_a/K_w) \frac{\partial c}{\partial t} = \frac{\partial}{\partial z} \left[(D + D_a/K_w) \frac{\partial c}{\partial z} \right] - (q + q_a/K_w) \frac{\partial c}{\partial z} \quad (3.10)$$

In the numerical model used here, the more general form (3.7) is used because cases are considered with nonisothermal conditions, hence spatially and temporally variable K_w . Also, the iterative solution of this mixed form numerically conserves mass (Celia et al., 1990).

The land-surface boundary condition used here is a specified concentration in the air phase, which corresponds to a specified water-phase concentration by the equilibrium assumption

$$c(t) = K_w C_a(t) \quad z = 0 \quad (3.11)$$

where C_a is the atmospheric concentration. The bottom boundary condition is no-flow for the case of $q=0$, or natural outflow by advection alone if flow is occurring:

$$\frac{\partial c}{\partial z} = 0 \quad z = L \quad (3.12)$$

Cook and Solomon (1995) solved this transport equation for several cases with different moisture content distributions, water fluxes, and uniform temperatures. In all cases, the moisture content was assumed to be uniform in the unsaturated zone down to the water table, and then to change abruptly at the water table to the porosity. A more realistic representation of the moisture content distribution is possible by solving the one-dimensional flow equation and using computed moisture contents and fluxes in the transport equation solution.

3.2.2 Constitutive Relations

Water Flow

The moisture retention curve describes the relation between pressure head and moisture content. The simple model of van Genuchten (1980) is chosen here to represent the moisture retention curve:

$$\theta = \theta_r + \frac{\theta_s - \theta_r}{\left[1 + (-\alpha_\theta h)^n\right]^{1-1/n}} \quad (3.13)$$

where θ_s [-] is the saturated moisture content; θ_r [-] is the residual moisture content; α_θ [L⁻¹] and n [-] are empirical coefficients. By volume conservation, the air content is the total porosity, ϕ [-], minus the moisture content: $\theta_a = \phi - \theta$.

Unsaturated hydraulic conductivity is generally a nonlinear function of moisture content. The Mualem (1976) - van Genuchten (1980) constitutive relation is chosen for unsaturated hydraulic conductivity:

$$k_{rw} \equiv \frac{K}{K_s} = \theta_e^{1/2} \left[1 - (1 - \theta_e^{1/m})^m\right]^2 \quad (3.14)$$

where K_s [LT⁻¹] is the saturated hydraulic conductivity; k_{rw} [-] is the relative hydraulic conductivity, $m \equiv 1 - 1/n$; and θ_e [-] is the normalized moisture content:

$$\theta_e \equiv \frac{\theta - \theta_r}{\theta_s - \theta_r} \quad (3.15)$$

Two soils are considered here, a sandy loam and a silty loam. The parameters for the van Genuchten and Mualem constitutive models are listed in Table 3-2, and the corresponding moisture retention and relative hydraulic conductivity functions are shown in Figure 3-1.

Transport

The dispersion coefficients include the effects of molecular diffusion and macroscopic dispersion, caused by spatial variability in velocity, modeled as Fickian diffusion:

$$\begin{aligned} D &= \theta D_m + \alpha q \\ D_a &= \theta_a \tau D_g + \alpha_a q_a \end{aligned} \quad (3.16)$$

in which D_m [L²T⁻¹] is the effective diffusion coefficient in the porous medium; α [L] is the porous media dispersivity for the water phase; τ [-] is the air-phase tortuosity; D_g

Table 3-2. Moisture retention and unsaturated hydraulic conductivity parameters for van Genuchten - Mualem model of a sandy loam and silty loam

Parameter	Sandy Loam	Silty Loam
θ_s , saturated moisture content	0.35	0.35
θ_r , residual moisture content	0.149	0.149
α_θ , van Genuchten coefficient	0.5 m^{-1}	0.5 m^{-1}
n , van Genuchten coefficient	7	2
K_s , saturated hydraulic conductivity	100 m/yr	1 m/yr

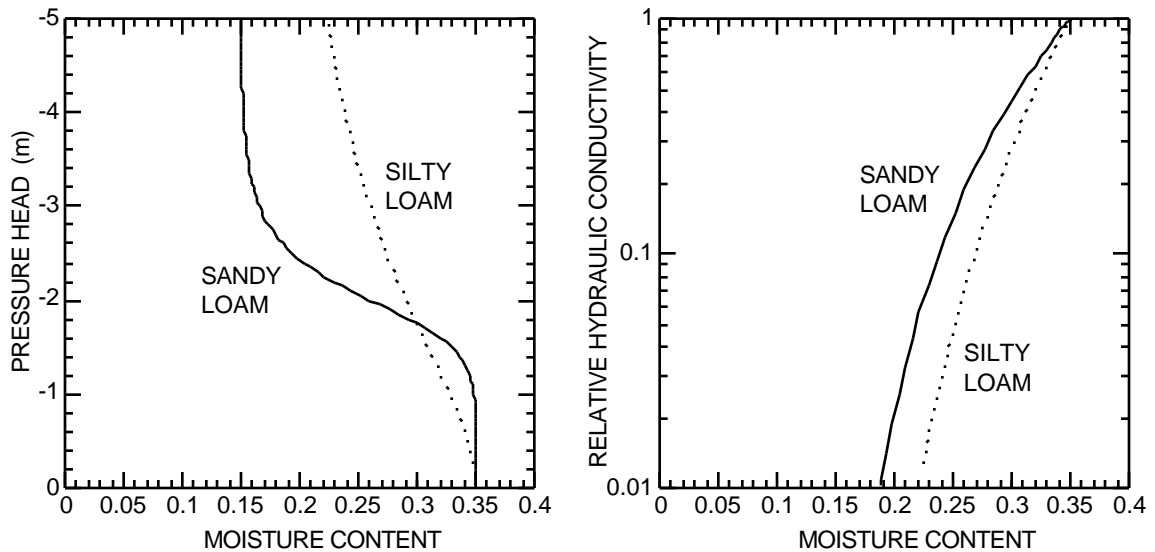


Figure 3-1 Moisture retention and relative unsaturated hydraulic conductivity for a sandy loam and a silty loam soil using Mualem - van Genuchten constitutive model.

$[L^2T^{-1}]$ is the free gas diffusion coefficient; and $\alpha_a [L]$ is the porous media dispersivity for the air phase. The effective water-phase diffusion coefficient includes the effects of tortuosity in the water phase. The air phase tortuosity is assumed to be a power law function of air content and total porosity (Millington, 1959):

$$\tau = \left(\frac{\theta_a}{\theta_a + \theta} \right)^2 \theta_a^{1/3} \quad (3.17)$$

Like many thermodynamic properties, the Henry's Law coefficient, that is the ratio of the concentration in water to the concentration in air, is a function of temperature (fig. 3-2). Cold water in equilibrium with air contains more CFC-11 than warm water. Warner and Weiss (1985) report the experimentally determined Henry's Law coefficient for CFC-11 as a function of temperature in degrees Kelvin ($^{\circ}\text{K}$):

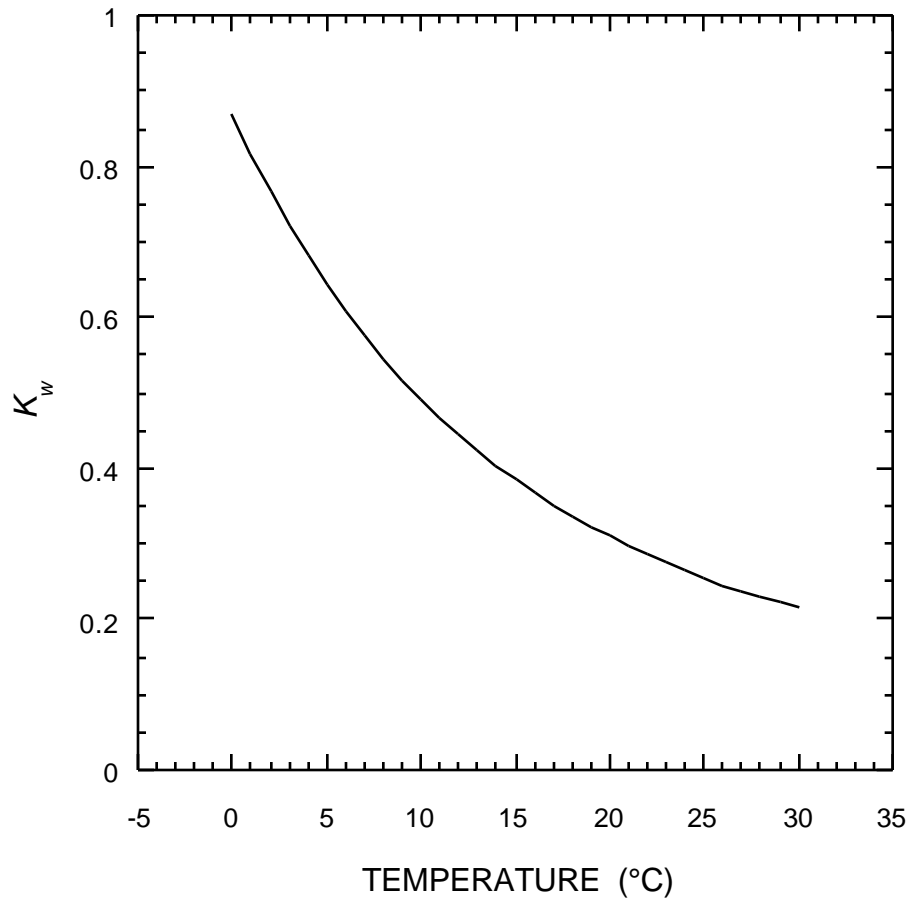


Figure 3-2 Henry's Law coefficient (K_w) for CFC-11; the ratio of the volumetric concentration in water having zero salinity to the volumetric concentration in air at sea level.

$$K_w = 0.0821 \text{ } ^\circ K \exp \left[a_1 + \frac{100 a_2}{^\circ K} + a_3 \ln \left(\frac{^\circ K}{100} \right) \right] \quad (3.18)$$

where a_1 , a_2 , and a_3 are gas-specific coefficients (volumetric form of Warner and Weiss, 1985). The units of the Henry's Law coefficient here are dimensionless: the mass in water per unit volume of water divided by the mass in air per unit volume of air.

The Henry's Law coefficient for CFC-11 as a function of temperature (fig. 3-2) is given by (3.18) with $a_1 = -134.1536$; $a_2 = 203.2156$, and $a_3 = 56.2320$ (Warner and Weiss, 1985). With these coefficients, the K_w value used by Cook and Solomon (1995) corresponds to an equilibration temperature of about 9.3 °C. Water in equilibrium with the atmosphere contains about 4 times more CFC-11 near freezing than it does at 30 °C. Warner and Weiss (1985) also present Henry's Law coefficients for CFC-12, and Bu and Warner (1995) present the CFC-113 coefficients.

3.2.2 Numerical Solution

The governing flow and transport equations are solved using standard finite-difference methods. The numerical model used here is a modified version of a flow and transport model developed by Michael A. Celia (personal communication, 1994; Celia and Binning, 1992). These modifications are primarily associated with incorporation of the air-phase transport terms into the transport equation solution. The numerical solution of the flow equation is based on the mixed form to guarantee numerical mass conservation (Celia et al., 1990). The flow equation solution is essentially that of Celia and others (1990) and is not described further here.

Approximation of the derivatives in the governing transport equation by centered differences in time and space on a uniformly-spaced finite-difference grid yields the numerical form for each node of the finite-difference grid:

$$\begin{aligned}
& \frac{(\theta + \theta_a/K_w)_i^{n+1} c_i^{n+1} - (\theta + \theta_a/K_w)_i^n c_i^n}{\Delta t} = \\
& \frac{1}{2\Delta z} \left[D_{i+1/2}^{n+1} \frac{c_{i+1}^{n+1} - c_i^{n+1}}{\Delta z} + (D_a)_{i+1/2}^{n+1} \frac{c_{i+1}^{n+1}/(K_w)_{i+1}^{n+1} - c_i^{n+1}/(K_w)_i^{n+1}}{\Delta z} \right. \\
& \left. - D_{i-1/2}^{n+1} \frac{c_i^{n+1} - c_{i-1}^{n+1}}{\Delta z} - (D_a)_{i-1/2}^{n+1} \frac{c_i^{n+1}/(K_w)_i^{n+1} - c_{i-1}^{n+1}/(K_w)_{i-1}^{n+1}}{\Delta z} \right] \\
& + \frac{1}{2\Delta z} \left[D_{i+1/2}^n \frac{c_{i+1}^n - c_i^n}{\Delta z} + (D_a)_{i+1/2}^n \frac{c_{i+1}^n/(K_w)_{i+1}^n - c_i^n/(K_w)_i^n}{\Delta z} \right. \\
& \left. - D_{i-1/2}^n \frac{c_i^n - c_{i-1}^n}{\Delta z} - (D_a)_{i-1/2}^n \frac{c_i^n/(K_w)_i^n - c_{i-1}^n/(K_w)_{i-1}^n}{\Delta z} \right] \\
& - \frac{q_{i+1/2}^{n+1} (c_{i+1}^{n+1} + c_i^{n+1}) - q_{i-1/2}^{n+1} (c_{i-1}^{n+1} + c_i^{n+1})}{4\Delta z} - \frac{q_{i+1/2}^n (c_{i+1}^n + c_i^n) - q_{i-1/2}^n (c_{i-1}^n + c_i^n)}{4\Delta z} \\
& - \frac{(q_a)_{i+1/2}^{n+1} [c_{i+1}^{n+1}/(K_w)_{i+1}^{n+1} + c_i^{n+1}/(K_w)_i^{n+1}] - (q_a)_{i-1/2}^{n+1} [c_{i-1}^{n+1}/(K_w)_{i-1}^{n+1} + c_i^{n+1}/(K_w)_i^{n+1}]}{4\Delta z} \\
& - \frac{(q_a)_{i+1/2}^n [c_{i+1}^n/(K_w)_{i+1}^n + c_i^n/(K_w)_i^n] - (q_a)_{i-1/2}^n [c_{i-1}^n/(K_w)_{i-1}^n + c_i^n/(K_w)_i^n]}{4\Delta z}
\end{aligned} \tag{3.19}$$

where i is the grid index, Δz is the uniform grid spacing, and $\Delta t = t^{n+1} - t^n$ is the time step. Identical equations for all nodes are assembled in a tri-diagonal matrix form, with appropriate modifications for flux or specified concentration boundary conditions at the top and bottom of the domain. The resulting matrix equation is solved directly at each time step using the Thomas algorithm for a tri-diagonal matrix equation. At each time step, the only unknowns are the water-phase concentrations at the new time level, $n+1$; all other terms are known from the previous time level or from the flow and temperature models.

3.2.3 Benchmark Simulation

A benchmark transport simulation is made to qualitatively compare the results of the modified transport model to those of Cook and Solomon (1995) for one of the cases they examined. General flow and transport parameters are in Table 3-3. Cook and

Solomon (1995) estimated the gas-phase diffusion coefficient for CFC-11 using the empirical equation of Slattery and Bird (1958). Using this same method for CFC-12 yielded an estimated value within 10 percent of the measured diffusion coefficient (Monfort and Pellegatta, 1991). The water table depth is 30 m and the moisture content of the unsaturated zone is uniformly 0.15. The bottom boundary condition, at $z = 40$ m, is no-flow for transport, and the top boundary condition is the specified CFC-11 concentration in the atmosphere. Cook and Solomon (1995) present profiles of CFC-11 concentration in the air phase above the 30 m deep water table for an isothermal case with $K_w = 0.51$.

Table 3-3. General flow and transport parameters used for CFC-11 transport simulations (after Cook and Solomon, 1995)

Parameter	Value
L, domain length	40 m
α , dispersivity in water phase	0.02 m
ϕ , total porosity	0.35
D_m , effective diffusion coefficient in water	0.03 m ² /yr
D_g , free gas diffusion coefficient	260 m ² /yr

Using parameter values identical or very similar to those of Cook and Solomon (1995), the profile of CFC-11 air-phase concentrations computed here (fig. 3-3) is essentially the same as their results (their fig. 2, p. 265). The CFC-11 concentration in the water has an identical shape but concentrations are reduced by the factor $K_w = 0.51$. Below the water table, only the water phase is present, and diffusion into the stagnant

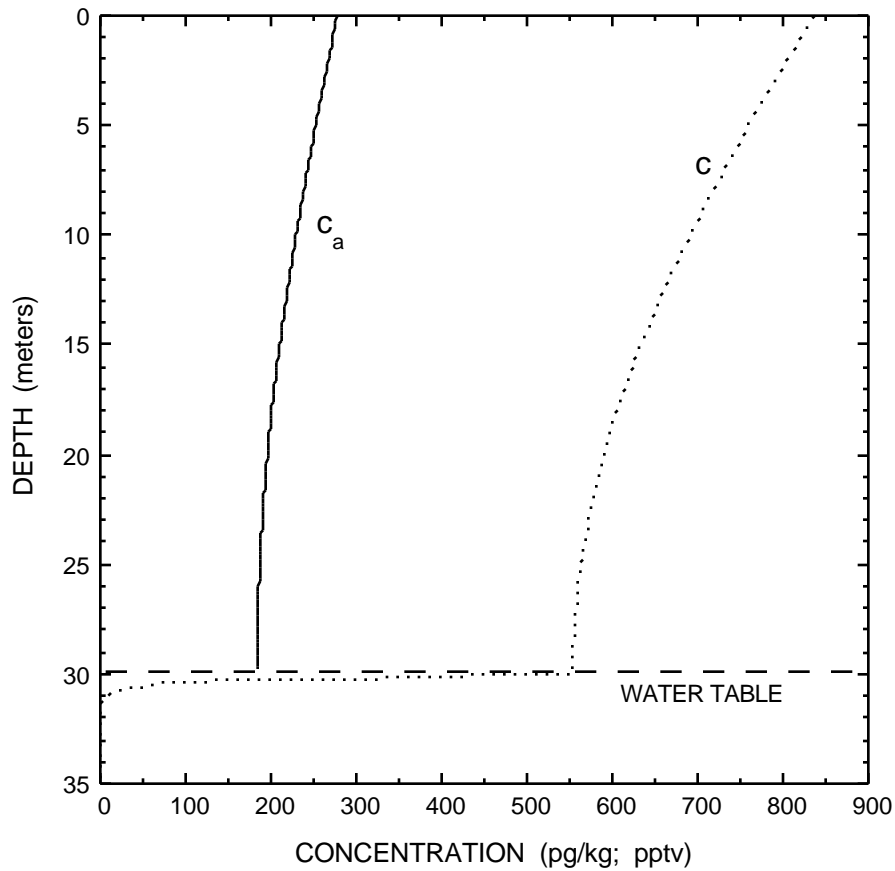


Figure 3-3 CFC-11 in water (c) and air (c_a) with depth, 1993, for unsaturated zone conditions of Cook and Solomon (1995, p. 265): uniform moisture and air content; isothermal; and water table at depth of 30 meters.

water is so slow that CFC-11 has diffused less than a meter below the water table. This result also reflects the very low atmospheric concentrations at the beginning of the simulation period in the 1940's.

3.3 Homogeneous Media

The simulations in this section are for the case of a homogeneous porous medium, as was considered by Cook and Solomon (1995) for their one-dimensional simulations.

3.3.1 Static Water

The impact of moisture retention above a water table on CFC-11 transport is examined for the case of a sandy loam (Table 3-2) and a water-table depth of 5 m. The porosity is assumed to be the same as the cases considered by Cook and Solomon (1995) to facilitate comparison with their results. The soil is near saturated for about 1 m above the water table because of the holding capacity of the fine-grained fraction of the soil. The associated reduction of air content significantly reduces the effective diffusion coefficient in the air phase (fig. 3-4), because the effective diffusion coefficient is the free coefficient times the product $\theta_a \tau$. These moisture-retention parameters are chosen to yield a relatively thick capillary fringe and a sharp reduction in moisture content above the capillary fringe.

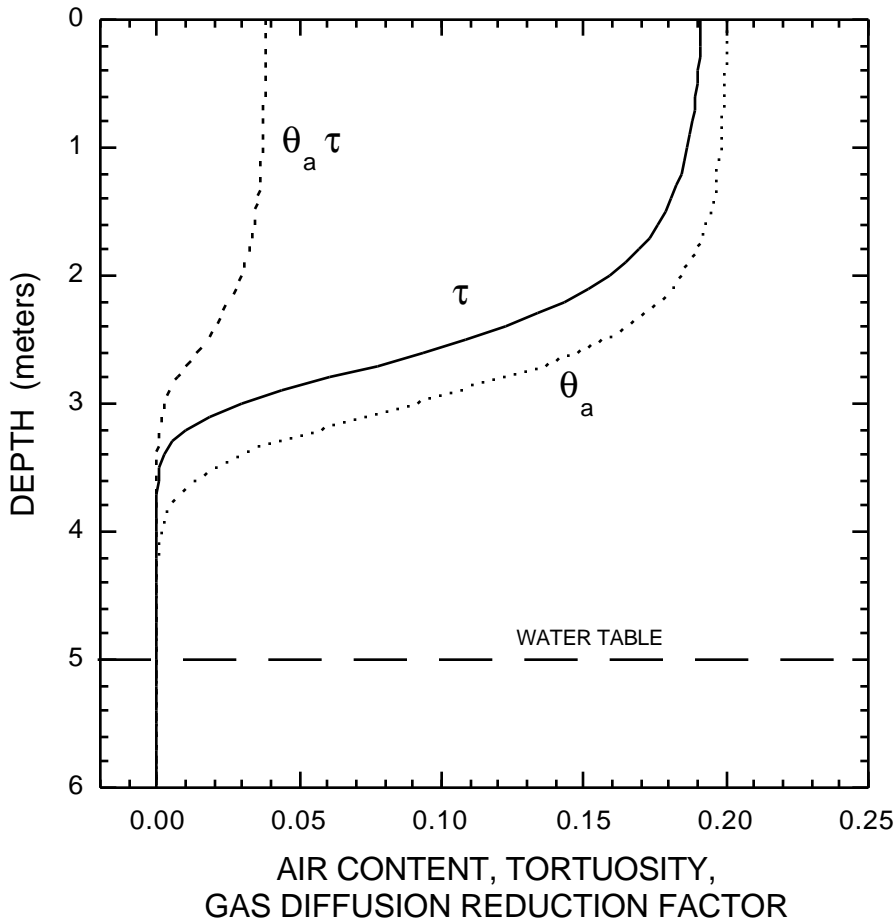


Figure 3-4 Air content (θ_a), tortuosity (τ), and their product versus depth for sandy loam moisture retention curve and water table depth at 5 meters.

The nonuniform moisture profile in the unsaturated zone reduces vertical transport (fig. 3-5). The primary effect is that downward gaseous diffusion stops at the capillary fringe, not at the water table. Without flow of water below the saturated zone, the concentrations at the water table are close to zero. The continuous variation of moisture content at the top of the capillary fringe results in more gradual changes in the CFC-11 profile, compared to the abrupt change in gradient for the case of Cook and Solomon (1995).

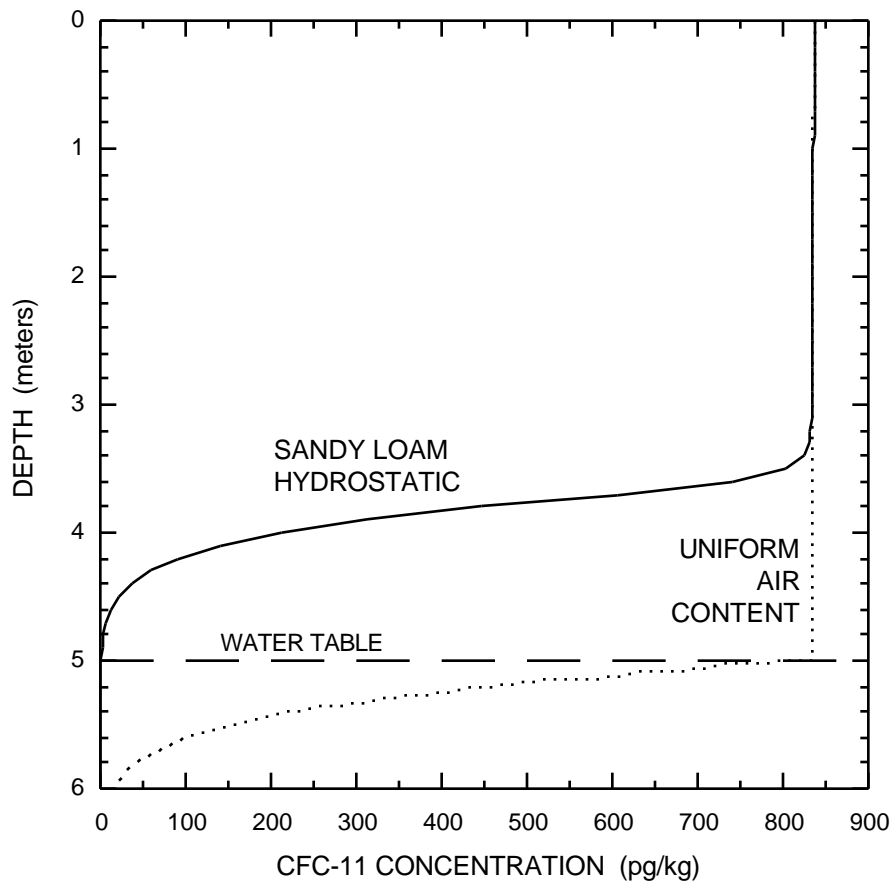


Figure 3-5 CFC-11 concentrations in 1993 versus depth for two no-flow cases having a water table at 5 meters depth: (a) uniform air content, and (b) sandy loam hydrostatic moisture retention curve.

3.3.2 Steady Water Flow

Cook and Solomon (1995) examine the impact of water flux rates on the unsaturated zone CFC-11 concentrations, but with a model having uniform moisture content in the unsaturated zone. A more realistic model of flow in the unsaturated zone leads to an even greater reduction in downward gaseous diffusion because the moisture contents are somewhat higher during downward flow.

Steady-state flow conditions are assumed with a downward water flux of $q = 0.3$ m/yr. Diffusion and dispersion in the saturated zone have little impact, because the

concentration gradients are small, hence advection is the dominant transport process for CFC-11 below the water table. The CFC-11 profile below the water table is essentially an image of the time history of CFC-11 concentrations in the atmosphere (fig. 3-6).

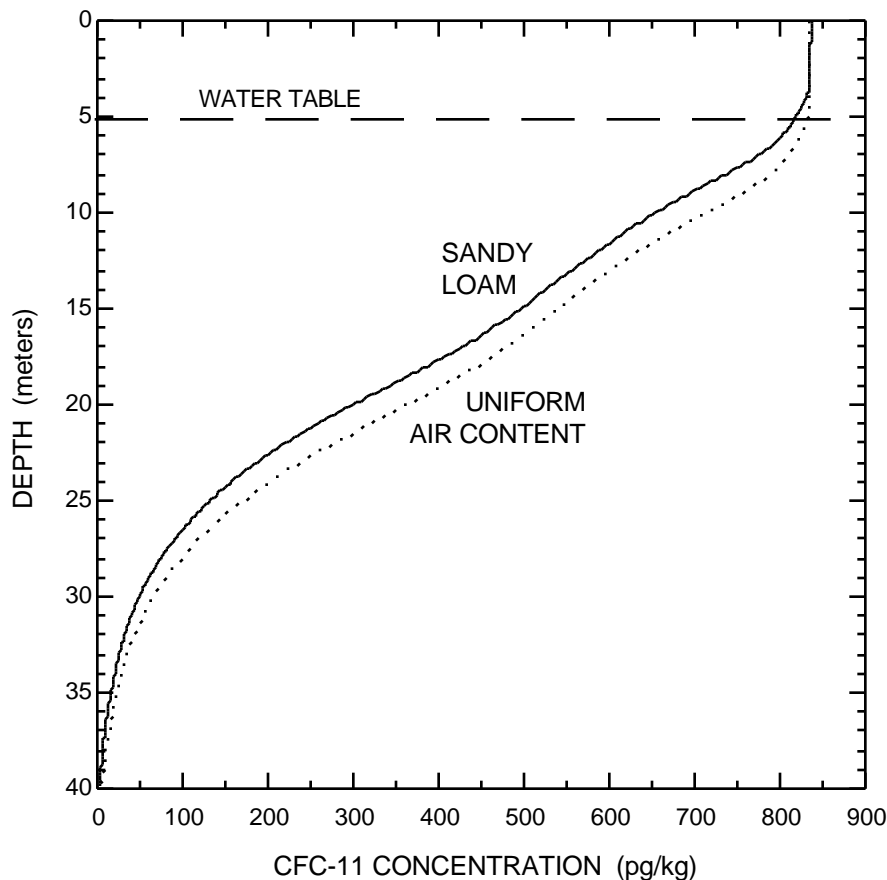


Figure 3-6 CFC-11 concentration versus depth with constant vertical flux of 0.3 m/yr and water-table depth of 5 m for cases (a) with uniform air content above the water table and (b) sandy loam moisture retention and hydraulic conductivity functions.

The increased moisture content above the water table for the sandy loam leads to a lag in the transport of CFC-11 into the saturated zone (fig. 3-6). This lag at the top of the saturated zone is propagated downward by the flowing water. The differences in CFC-11 concentrations at any location correspond to about 10 percent difference in apparent ages for the uniform moisture content and the sandy loam cases.

3.3.3 Seasonal Temperature Cycle

Because the Henry's Law coefficient for CFC-11 is a function of temperature, the transport of CFC-11 from the atmosphere to the water depends on temperature in the unsaturated zone. Cook and Solomon (1995) evaluated the effect of temperature on CFC-11 transport for isothermal cases with uniform temperature distribution. However, temperature is not uniform with depth in real soils, and near the land surface strong seasonal cycles occur due to the seasonal cycle in air temperature and solar radiation. In this section CFC-11 transport is examined under conditions of a seasonal temperature cycle.

Temperatures in the subsurface fluctuate seasonally near the land surface due to the annual cycle in air temperatures and solar radiation. A classic and simple model of the subsurface temperature profile is based on a sinusoidal annual temperature at the land surface and uniform heat conduction in the subsurface. Assuming that at infinite depth the subsurface remains at the mean annual temperature, and that the minimum surface temperature occurs on January 1 ($t=0$ yr), then the temperature as a function of depth and time of year can be written (Hillel, 1982)

$$T(z, t) = \bar{T} + A \sin [2\pi(t - 0.25\text{yr} - z/d)] \exp(-z/d) \quad (3.20)$$

where t is the time of year in years, \bar{T} is the mean annual temperature, A is the amplitude of the land surface temperature cycle, and d [L] is the damping depth defined as

$$d \equiv \left(\frac{2D_h}{2\pi \text{yr}^{-1}} \right)^{1/2} \quad (3.21)$$

where D_h [L^2T^{-1}] is the uniform thermal diffusivity. The denominator in (3.21) is the frequency of the temperature cycle in radians per time, in this case for an annual cycle. For the simulations here, the thermal diffusivity is $D_h = 27.2 \text{ m}^2/\text{yr}$, corresponding to a wet sand (Hillel, 1982), and the damping depth is $d = 2.94 \text{ m}$. The mean annual temperature is taken as $9.2681 \text{ }^\circ\text{C}$, and the temperature amplitude is equal to the mean annual temperature. Thus, the annual cycle in temperature at the land surface exhibits a

minimum of 0 °C on 1 January and a maximum of 18.54 °C on 1 July. Transport and storage of heat in the subsurface causes the temperature amplitude to drop off with depth, and causes the temperatures at depth to lag behind the surface forcing (fig. 3-7).

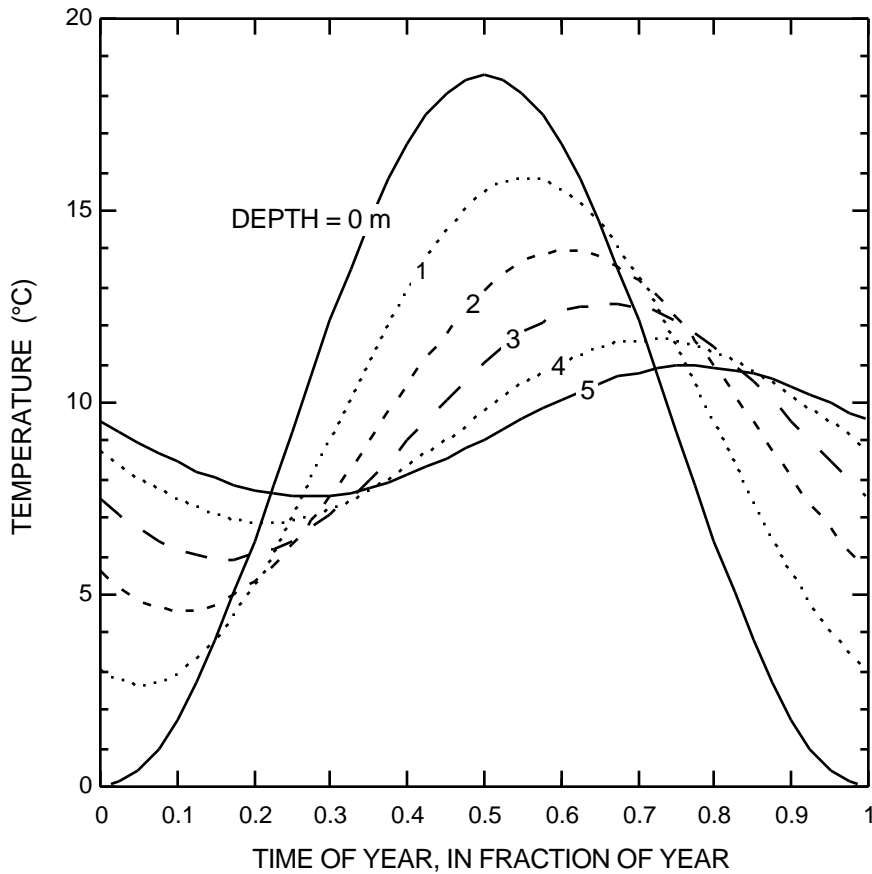


Figure 3-7 Annual temperature cycle for analytical model with sinusoidal surface temperature (mean and amplitude of 9.2681 °C) and uniform thermal diffusivity ($D_h = 27.2 \text{ m}^2/\text{yr}$).

The amount of CFC-11 partitioned between the air and water phases changes as the temperature changes, hence the seasonal cycle in temperature within the unsaturated zone causes a seasonal cycle in the Henry's Law coefficient. Furthermore, the lag in temperature with depth yields a spatially variable K_w . For example, on 1 January the land surface temperature is at its minimum and K_w is at its maximum at this location (fig. 3-8).

At this time, temperatures beneath the land surface are decreasing from the higher temperatures of the summer period. As K_w changes in time, the partitioning between air and water is assumed to adjust instantly. As temperatures are dropping, CFC-11 moves from the air phase to the water phase, and vice versa. This re-partitioning can only occur where both phases are present.

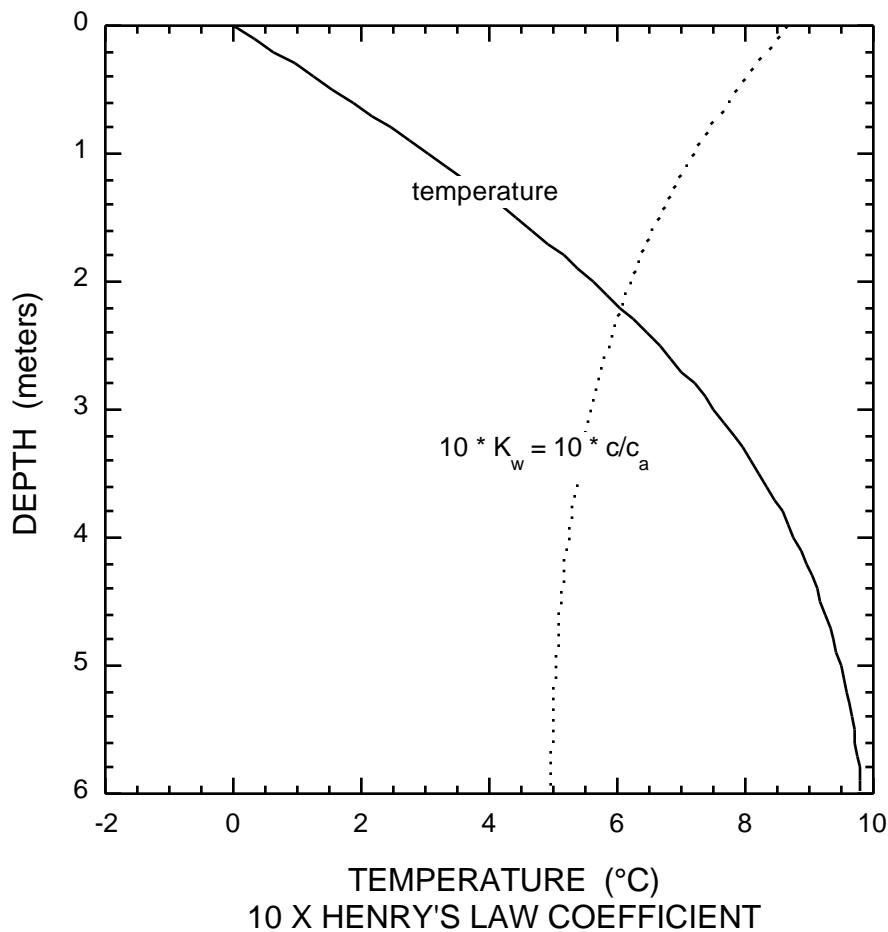


Figure 3-8 Temperature and Henry's Law coefficient versus depth on 1 January 1993 for nonisothermal conditions simulated by analytic model.

Above the capillary fringe, CFC-11 concentrations in water exhibit a strong seasonal cycle that corresponds to, but lags, the temperature cycle (fig. 3-9). At depths of 3 and 3.5 m, the water concentration mirrors the temperature cycle, with maximum

concentrations slightly lagged from minimum temperatures. This lag is due to the diffusion in the air phase within the unsaturated zone. For example, at 3.5 m, as the soil cools, CFC-11 is removed from the air phase and added to the water phase. This reduction in air-phase concentrations will lead to increased diffusion downward from the land surface, except that temperatures above this depth are even cooler. These cooler temperatures at shallower depths mean that CFC-11 air-phase concentrations are depleted, hence air-phase concentrations gradients cause upward diffusion. After the temperature minimum at 3.5 m, shallower depths are warmer hence have excess CFC-11 in the air phase which leads to increased air- and water-phase concentrations by air-phase

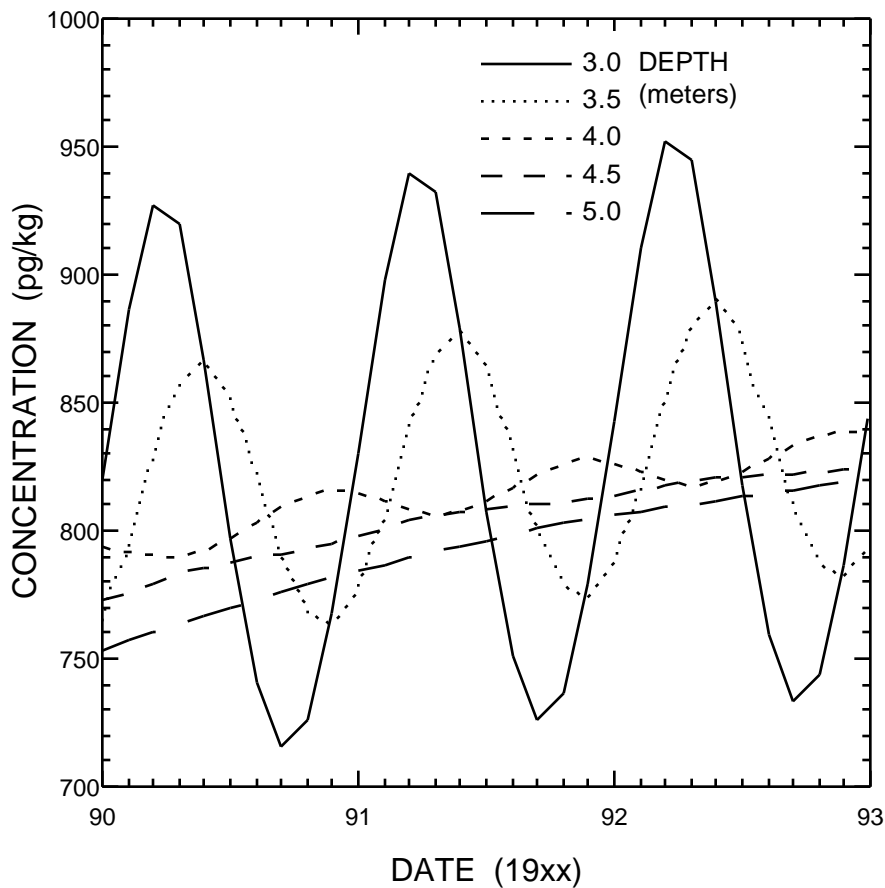


Figure 3-9 CFC-11 concentrations versus time from 1990 to 1993 for water table at depth of 5 m and steady water flux of 0.3 m/yr, under nonisothermal conditions.

diffusion downward. The direction of air-phase diffusion is changing throughout the year because the temperature cycles lead to large fluctuations in air-phase concentrations, relative to the gradual long-term atmospheric trend.

Within and below the capillary fringe, the volume of the air phase is small, hence water concentrations are not significantly affected by re-partitioning. Concentration cycles in this zone correspond to advective transport of water which carries the concentration cycle at the top of the capillary fringe down into the saturated zone. The approximately 0.5 yr lag in concentrations between 3.5 and 4 m depth is not the same as the temperature lag, but is close to the advective travel time between these depths, which is approximately $0.5 \text{ m} / (q / \theta) = 0.5 \text{ m} / (0.3 \text{ m/yr} / 0.35) = 0.58 \text{ yr}$.

The temporal cycle in CFC-11 concentrations in water is lagged compared to the temperature cycle above the capillary fringe, while below the capillary fringe the concentration cycle is approximately the cycle at the top of the capillary fringe advected downward by the flowing water. The break between these two different regimes is more specifically controlled by the magnitude of the effective diffusion coefficient, which is the sum of the air and water phase diffusion coefficients, weighted by the air and moisture contents (fig. 3-10). Where this term is large, the concentration cycle is controlled by temperature fluctuations, re-partitioning, and air phase diffusion. Where the effective diffusion coefficient is small, the concentration cycle is controlled by advection in the water and further dampening by water phase diffusion and dispersion.

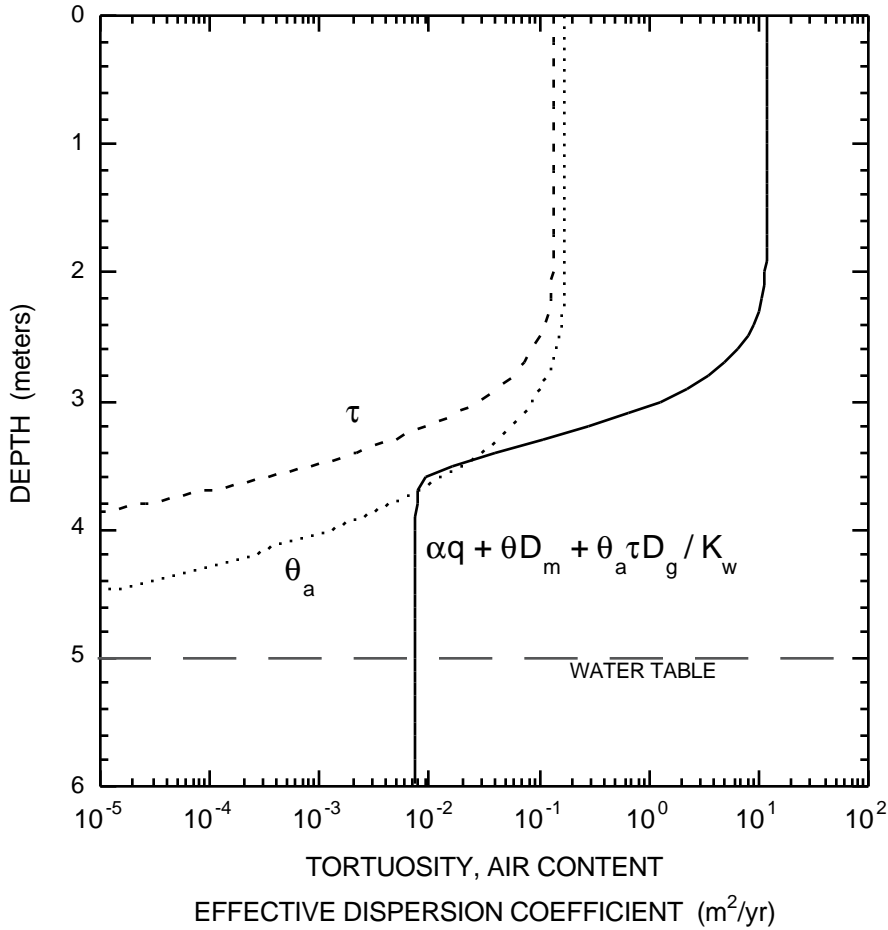


Figure 3-10 Air content, moisture content, and effective dispersion coefficient versus depth for sandy loam with water table at depth of 5 m and steady flow of 0.3 m/yr.

Although the water- and air-phase concentrations of CFC-11 fluctuate under nonisothermal conditions, the resulting saturated-zone concentrations are essentially unaffected by these fluctuations (fig. 3-11). Air-phase diffusion is the dominant transport mechanism from the land surface to the top of the capillary fringe, and temperature fluctuations are not large at that depth.

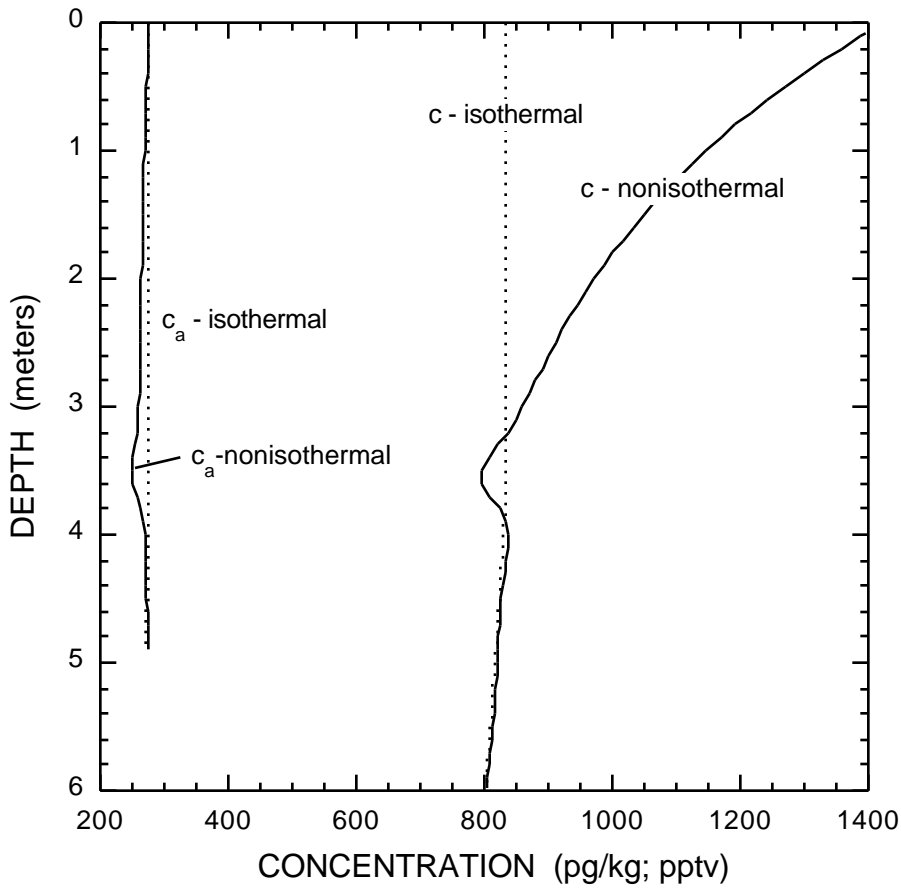


Figure 3-11 CFC-11 concentration versus depth on 1 January 1993 for water table at depth of 5 m and steady water flux of 0.3 m/yr. Results for isothermal and nonisothermal conditions are shown.

If the water table is at a depth of 1 m, instead of 5 m, then the saturated-zone concentrations are impacted significantly by nonisothermal conditions. For the same water flux rate, 0.3 m/yr, but with a water table depth of 1 m, the saturated-zone concentrations are about 10 percent higher under nonisothermal conditions (fig. 3-12).

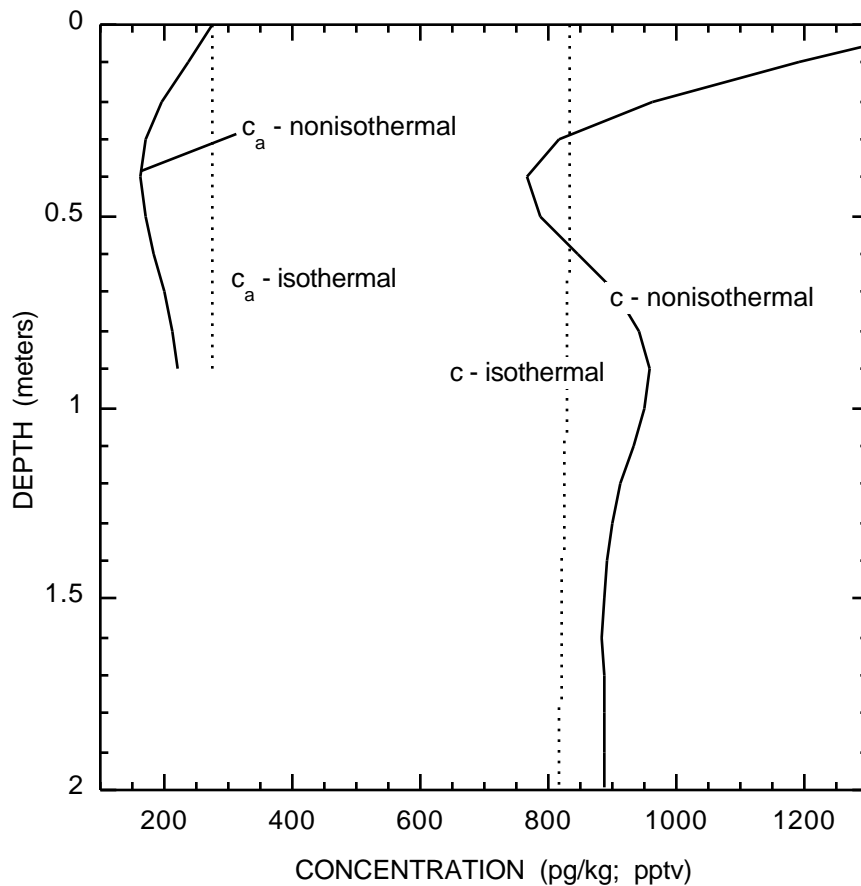


Figure 3-12 CFC-11 concentration versus depth on 1 January 1993 for water table at depth of 1 m and steady water flux of 0.3 m/yr. Results for isothermal and nonisothermal conditions are shown.

The fluctuations of water-phase concentrations within the unsaturated zone in the case of a water-table depth of 1 m do not correspond to the temperature fluctuations (fig. 3-13). Rather, the water-phase concentration at the land surface fluctuates according to the land-surface temperature, and that fluctuation is advected down by the flow of water, with subsequent dampening by dispersion. The capillary fringe extends to the land surface in this case, and air-phase transport is negligible.

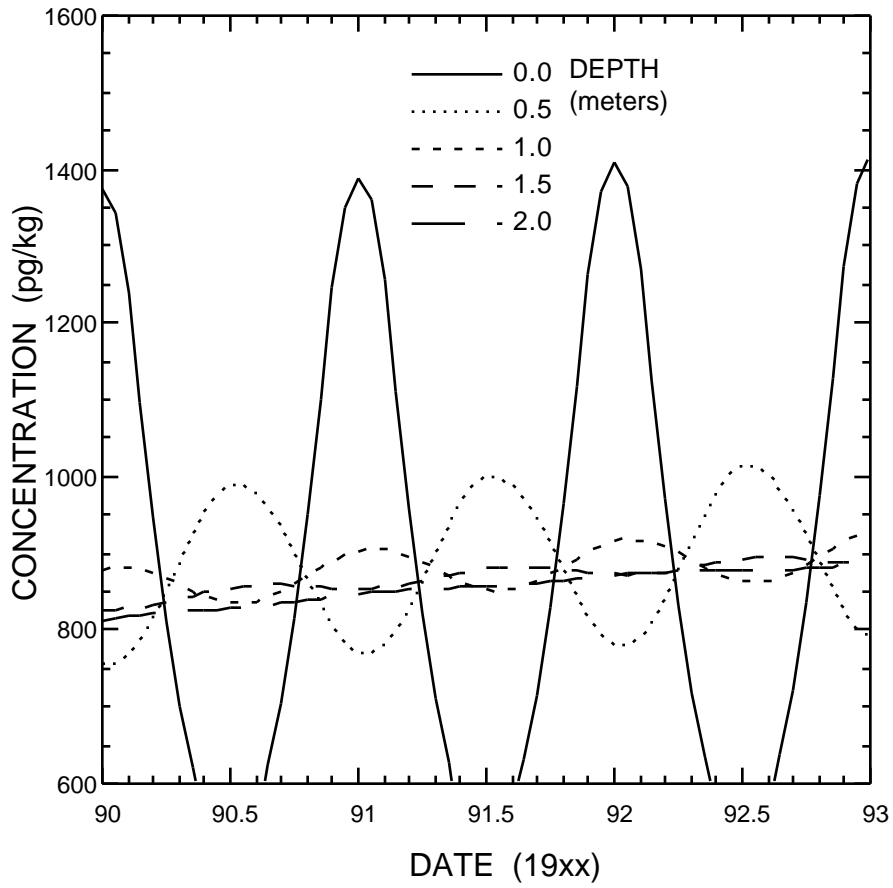


Figure 3-13 CFC-11 concentrations versus time from 1990 to 1993 for water table at depth of 1 m and steady water flux of 0.3 m/yr, under nonisothermal conditions.

3.4 Layered Soil

Natural porous media are not homogeneous, and inhomogeneities can have significant effects on flow and transport. Simulations for conditions analogous to those examined in previous sections are re-run with a simple layered porous medium to examine some of these effects. The majority of the porous-media system is the sandy loam of the previous section. A silty-loam layer occurs in the soil column between 1 and 2 m below the land surface. As described in the previous section on constitutive relations, this silt loam has a lower saturated hydraulic conductivity than the sandy loam, and retains more moisture at higher negative pressures.

3.4.1 Static Water

Under static-water conditions, the pressure and moisture-content distribution is independent of hydraulic conductivity. Inclusion of the silty layer in the column has no effect on pressure in this case, but leads to higher moisture contents within the layer compared to the homogeneous sandy loam case. This is because of the moisture-retention characteristics of the silty loam; it holds more water at an equivalent pressure. However, the moisture content is not close enough to saturation to significantly impact air-phase diffusion. Hence, the water-phase concentrations of CFC-11 are essentially the same as the homogeneous case (fig. 3-14).

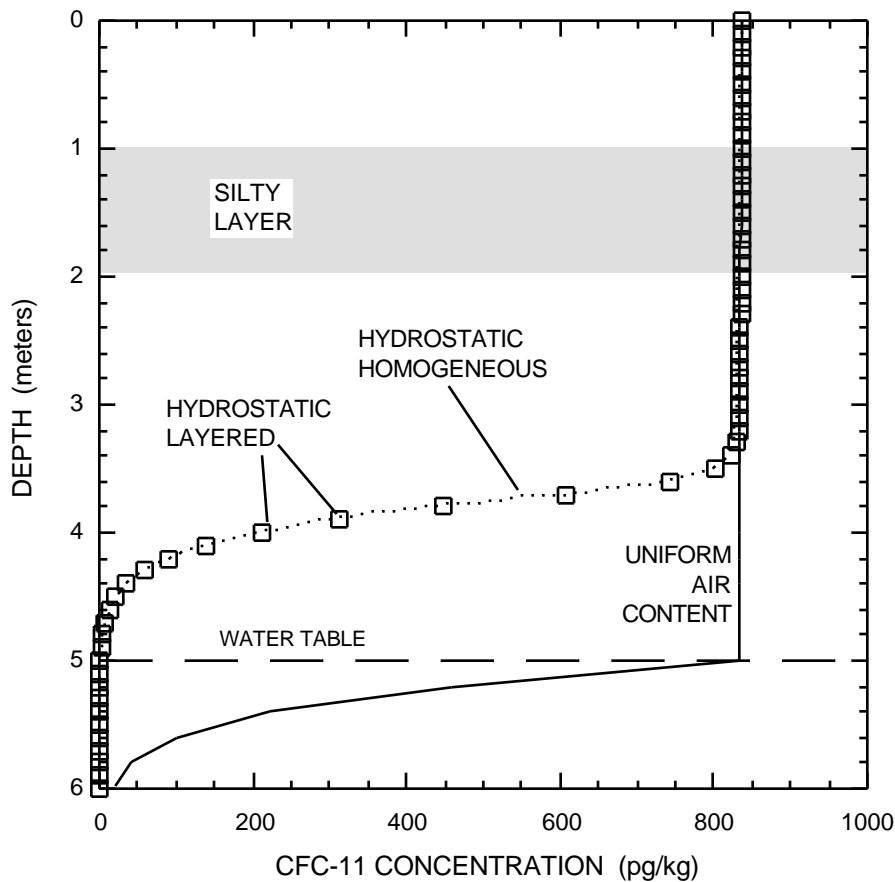


Figure 3-14 CFC-11 concentrations versus depth for case having water table at 5 m depth and no flow for cases (dashed) uniform moisture content, (solid) homogeneous sand loam, and (symbols) layered sand with a silt layer between 1 and 2 m depth.

3.4.2 Steady Water Flow and Seasonal Temperature Cycle

The silt layer has more effect on transport during steady flow because the hydraulic conductivity of the silt layer impedes flow and increases moisture contents in the unsaturated zone above the water table (fig. 3-15). CFC-11 concentrations at the water table (5 m) are lower for both isothermal and nonisothermal conditions, when compared to the results for the same conditions with a homogeneous porous medium (fig 3-11). For the previous simulation of a water table at 5 m depth in a homogeneous column, the impact of nonisothermal conditions on the concentrations at the water-table

are insignificant. However, nonisothermal conditions cause a noticeable increase in concentrations at the water-table in the layered case.

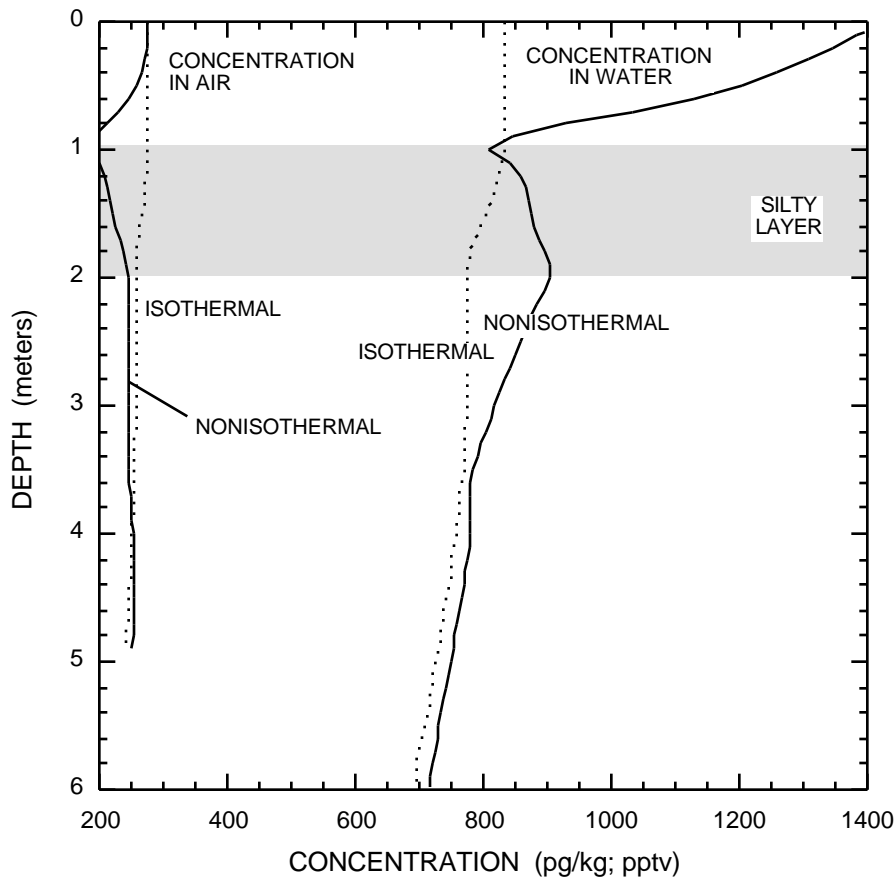


Figure 3-15 CFC-11 concentrations versus depth for case having water table at depth of 5 m, steady flow of 0.3 m/yr, and silt layer between 1 and 2 m depth for cases (dashed) isothermal, and (solid) nonisothermal conditions.

The specified flow rate of 0.3 m/yr is close to the saturated hydraulic conductivity of the silt material (1.0 m/yr). Hence saturations must be high in this layer and pressures must be close to zero at the top of the silt layer. Pressures will be close to zero in the sand layer as well because pressure is continuous. At the particular pressures simulated, the sand is more saturated than the silt at the top of the silt layer (see fig. 3-1), and hence the air phase content is lower, the tortuosity is lower, and the overall effective dispersion

coefficient is lower (fig 3-16). This high moisture content limits air-phase diffusion and results in lower water-table concentrations.

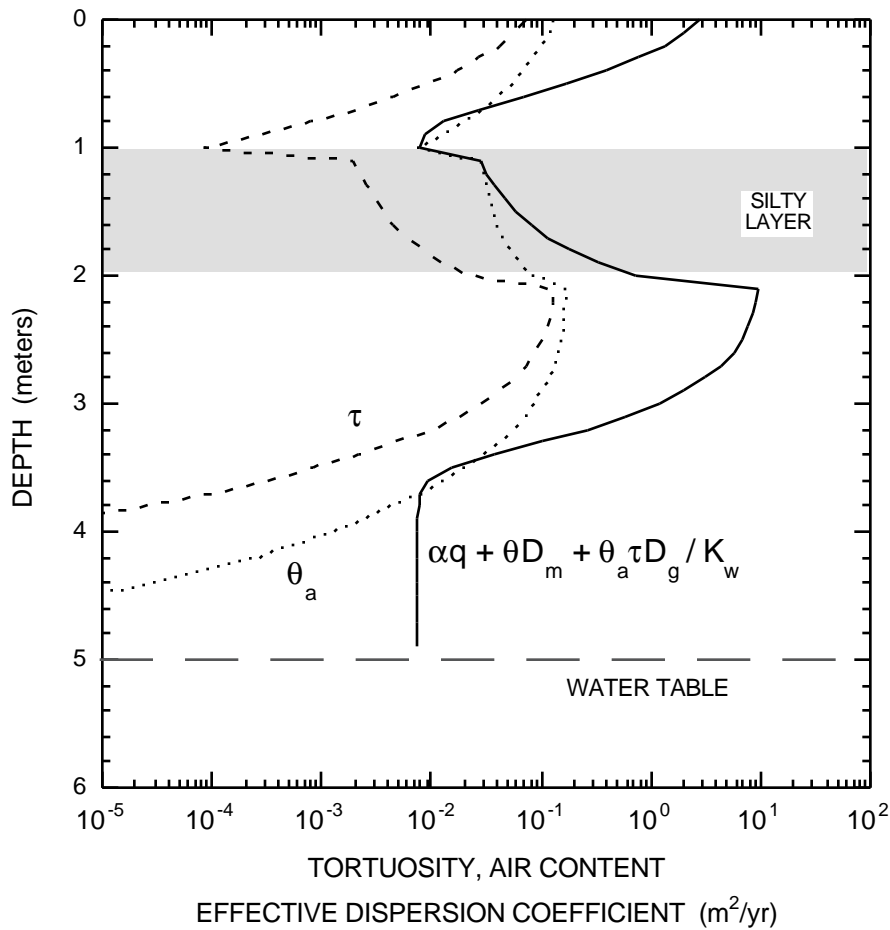


Figure 3-16 Air content, moisture content, and effective dispersion coefficient versus depth for layered case with water table at depth of 5 m and steady flow of 0.3 m/yr.

Nonisothermal conditions lead to noticeably higher water-table concentrations for this layered case compared to the isothermal conditions. This result is in contrast to the corresponding homogeneous case, in which temperature fluctuations had little impact on water-table concentrations for the 5 m deep water table (fig. 3-11). In the layered case, the high moisture content at the top of the silt layer isolates the air at greater depths from the near-surface air. Transport from this point downward is essentially controlled by the

water-phase concentration, and not the air-phase concentration, because diffusion in the air phase is so small. Of course, the water-phase concentration at this depth varies seasonally with temperature because the temperature is fluctuating at this depth.

3.5 Henry's Law Coefficient for Recharge

To determine a date of isolation from the atmosphere from CFC concentrations in a ground-water sample, the equilibration temperature between the sampled water and the atmosphere must be known. Equilibration temperatures are typically estimated from actual air temperature, taking the annual average, or from concentrations of other dissolved gases in the sample, such as nitrogen and argon (see Chapter 4).

The extent to which water-table concentrations are affected by fluctuating temperature is determined not by the extent of temperature fluctuations at the water table, but the extent of temperature fluctuations at the shallowest depth where air-phase diffusion is negligible; that is where the moisture content is near saturation. The air phase below this point is essentially isolated from the atmosphere, and deeper migration is controlled by the water-phase concentration there, because the air phase is essentially absent. If the temperature is fluctuating at this depth, then the water-phase concentration fluctuates as well because of equilibrium exchange with the overlying air column.

In the homogeneous column case, fluctuating temperature had no impact on water-table concentrations for a 5 m-deep water table. Air-phase diffusion is high down to the top of the capillary fringe (at about 4 m), and temperature fluctuations there are small, ranging from about 7 to 11.5 °C (fig 3-17). The average Henry's Law coefficient, 0.513, is very close to the Henry's Law coefficient at the average temperature, 0.510; a difference of about 0.6 percent.

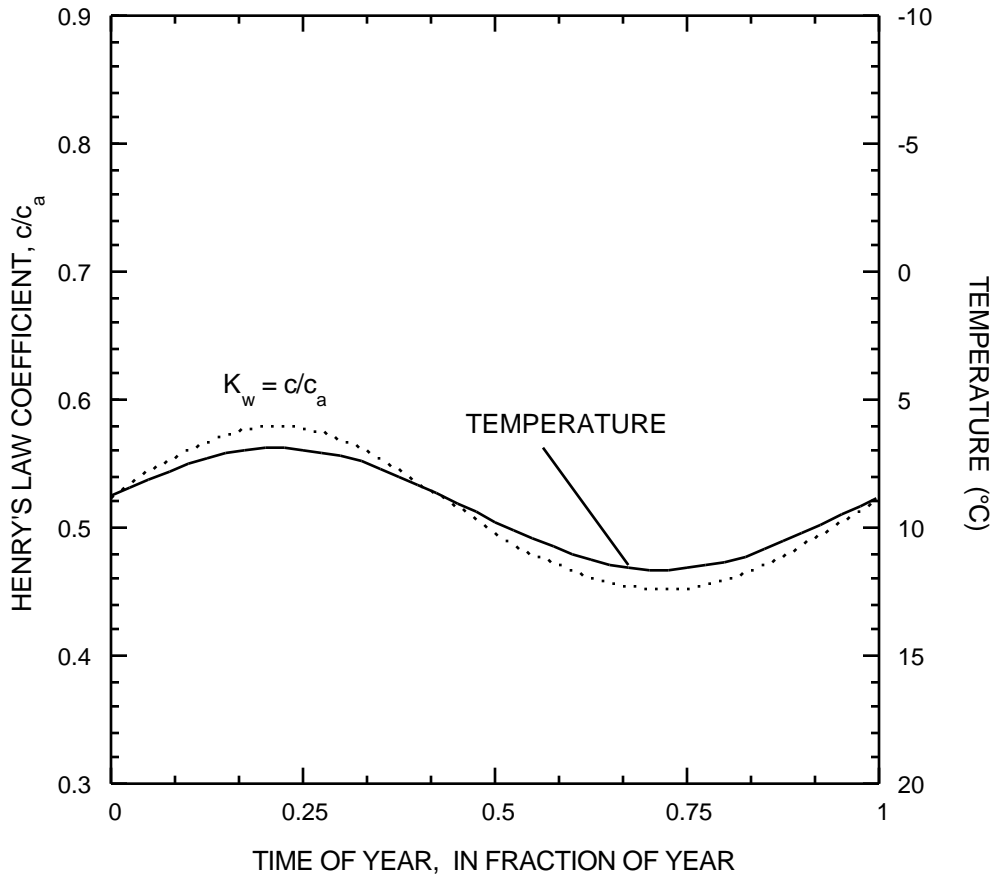


Figure 3-17 Annual cycle in temperature and Henry's Law coefficient at 4 m depth.

If the water table is close to the land surface, then temperature fluctuations at the top of the capillary fringe will be large. In this case, the average Henry's Law coefficient at that point will be higher than the Henry's Law coefficient at the average temperature. This is illustrated here by the case of the homogeneous column with the water table at a depth of only 1 m. In this case, for the sand-loam soil, the column is essentially saturated all the way to the land surface. The average Henry's Law coefficient, 0.554, is over 8 percent higher than the Henry's Law coefficient at the average temperature, 0.510 (fig. 3-18).

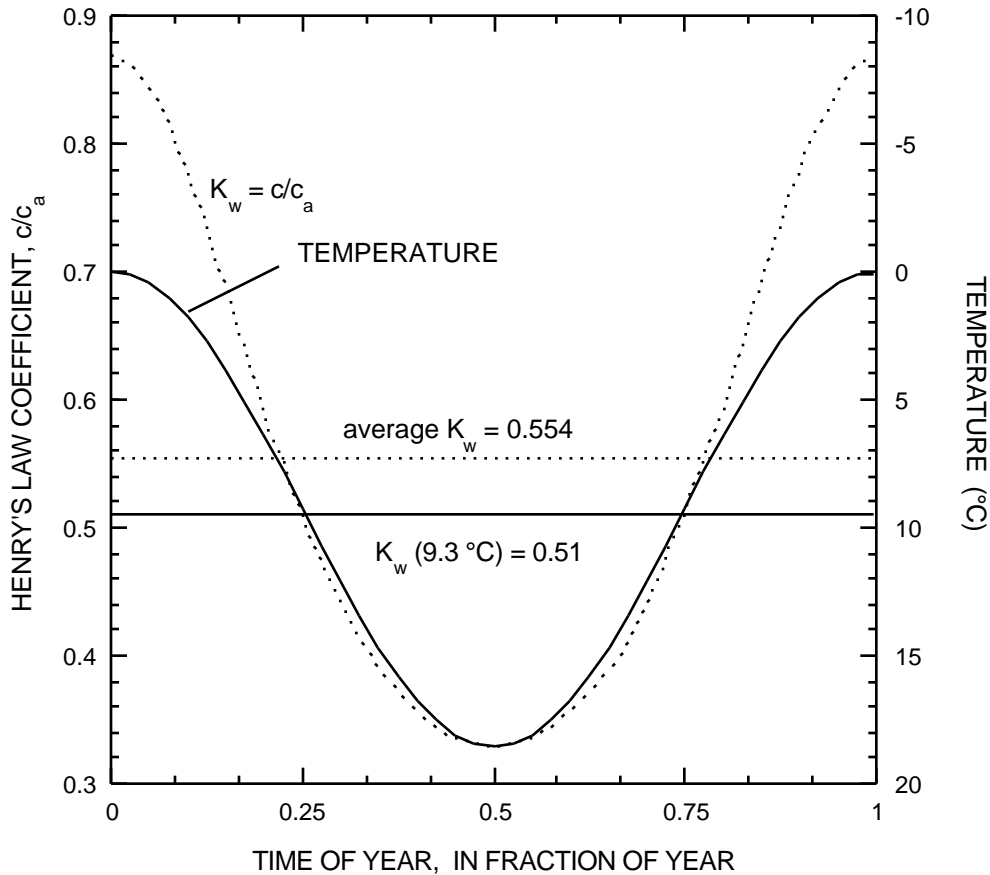


Figure 3-18 Annual cycle in temperature and Henry's Law coefficient at land surface.

The average Henry's Law coefficient at the highest nearly-saturated depth will be higher than the Henry's Law coefficient at the average temperature, because of the shape of the $K_w(^{\circ}\text{C})$ function. The magnitude of this difference depends on the temperature range experienced at that location. The best method to estimate this quantity would be to measure the temperature monthly or more frequently, compute the corresponding Henry's Law coefficients, and take the annual average K_w .

The same nonlinear effect shown here for CFC-11 will also impact CFC-12 and CFC-113 concentrations to about the same extent. The temperature dependence of the Henry's Law coefficients from CFC-113 and CFC-12 have essentially the same relative shape as the CFC-11 function (fig. 3-19), hence will be affected in much the same way.

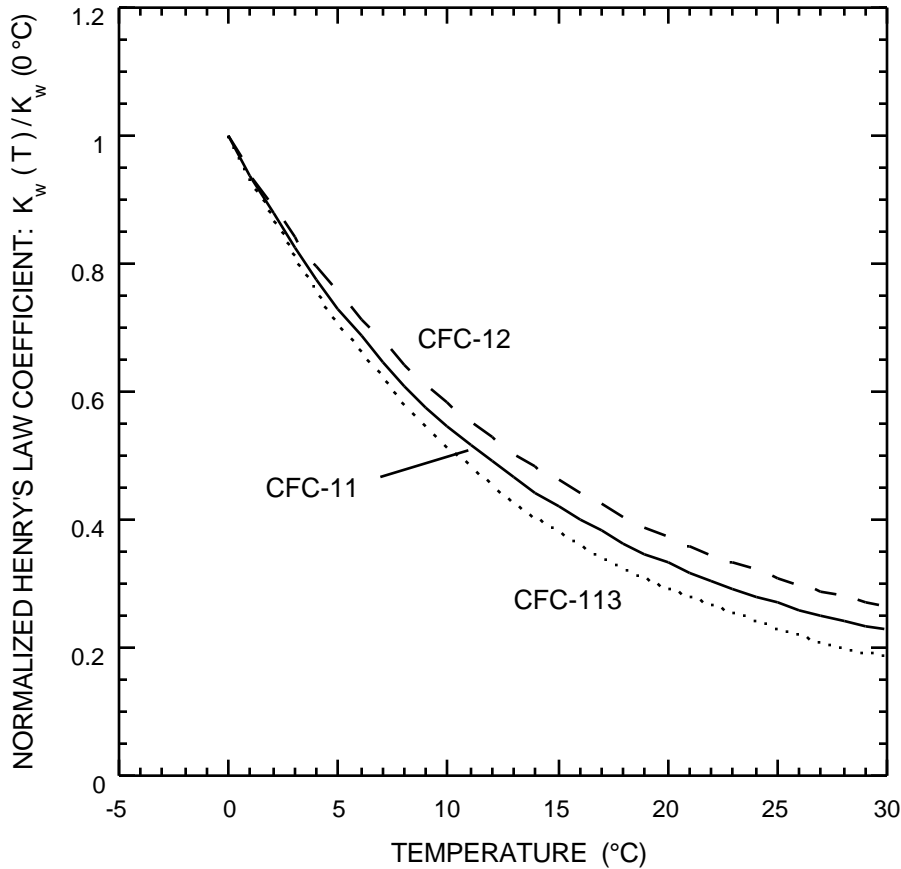


Figure 3-19 Henry's Law coefficients for CFC-11, CFC-12, and CFC-113, normalized by their respective values at $T = 0^\circ\text{C}$, as a function of temperature.

The saturations of most gases in water are nonlinear functions of temperature. Hence, this effect should also be observed to some extent in noble gas concentrations. The standard methods for estimating recharge temperature from these gas concentrations assume isothermal conditions, which may be expected to yield erroneous results for cases where isolation from the atmosphere occurs at shallow depth. If the Henry's Law coefficient is only weakly dependent on temperature, or the temperature range is small, then these effects can be safely ignored.

3.6 Summary

Transport of CFC-11 (and other gases) from the land surface to the saturated zone is characterized by rapid air-phase diffusion in the unsaturated zone down to a depth where the moisture content is nearly saturated. Below this point, transport is dominated by advection in flowing water, with minor diffusion and dispersion. Horizontal flow, which is not considered here, dominates solute advection in the saturated zone in many cases. CFC-11 concentrations at the water table will generally reflect a lag from atmospheric levels due to air-phase diffusion and advection through the capillary fringe. The former is small in cases with shallow water tables and increases with water-table depth, while the latter depends primarily on the moisture retention function and the recharge rate, and is independent of water-table depth.

At some distance above the water table, moisture contents are sufficiently high that air-phase diffusion no longer dominates vertical transport. Usually this would be at the top of the capillary fringe. However, in layered or inhomogeneous media, zones may exist well above both the water table and the capillary fringe where moisture contents are near saturation.

Temperature fluctuations will have an impact on CFC-11 transport to the water table only if temperature fluctuations are large ($> 5^{\circ}\text{C}$) at the shallowest point where air diffusion is negligible. In these cases, CFC-11 concentrations at the water table will be higher than those corresponding to isothermal conditions. This increase is due to the nonlinear relation between the Henry's Law coefficient and temperature. For the cases considered here, CFC-11 concentrations at the water table increased at most by about 10 percent for nonisothermal cases, compared to isothermal cases at the same average temperature.

CFC-11 concentrations within the unsaturated zone fluctuate throughout the year at depths where the temperature fluctuates. Hence, diffusion gradients can change

direction during the course of a year. Fluctuations in concentration at the top of the (nearly) saturated zone are propagated downward by the flowing water, and water-phase dispersion will dampen the fluctuations as advection progresses. These fluctuations in the unsaturated zone can cause air-phase concentrations to fluctuate around atmospheric levels by several 10's of percent.

Ideally, average Henry's Law coefficients can be computed from measured temperatures if fluctuating temperatures are significant at the top of the capillary fringe. The difference between the average Henry's Law coefficient and the Henry's Law coefficient at the average temperature is small if the temperature range is small. The relative temperature dependence of Henry's Law coefficients for CFC-12 and CFC-113 are similar to that of CFC-11, hence similar results would be expected for those gases. Fluctuating temperatures will have similar impacts on water-phase concentrations of other gases that have a nonlinear functional dependence on temperature, and the impact will depend on the sensitivity of the Henry's Law coefficient to the temperature.

The impact of fluctuating temperatures on CFC-11 concentrations in ground water is likely to be small in most cases. However, differences in computed atmospheric concentrations translate directly into age-estimation errors. In extreme cases, age-dating errors of 10 percent, or about 5 years, would be expected for cases having 20 °C temperature fluctuations at the top of the capillary fringe.

3.7 References

- Bu, W., and M.J. Warner, 1995, Solubility of chlorofluorocarbon 113 in water and seawater, *Deep Sea Research*, v. 42, no. 7, p. 11512-1161.
- Celia, M.A., and Binning, Philip, 1992, A mass conservative numerical solution for two-phase flow in porous media with application to unsaturated flow: *Water Resources Research*, v. 28, no. 10, p. 2819-2828.
- Celia, M.A., Bouloutas, E.T., and Zarba, R.L., 1990, A general mass-conservative numerical solution for the unsaturated flow equation: *Water Resources Research*, v. 26, no. 7, p. 1483-1496.
- Cook, P.G., and D.K. Solomon, 1995, Transport of atmospheric trace gases to the water table: Implications for groundwater dating with chlorofluorocarbons and krypton 85, *Water Resources Research*, v. 31, no. 2, p. 263-270.
- Hillel, Daniel, 1982, *Introduction to Soil Physics*: Academic Press, Orlando, Fla., 364 p.
- Millington, R.J., 1959, Gas diffusion in porous media, *Science*, v. 130, p. 100-102.
- Montfort, J.-P., and Pellegatta, J.-L., 1991, Diffusion coefficients of the halocarbons CCl₂F₂ and C₂Cl₂F₄ with simple gases: *Journal Chemical Engineering Data*, v. 36, p. 135-137.
- Mualem, Y., 1976, A new model for predicting the hydraulic conductivity of unsaturated porous media: *Water Resources Research*, v. 12, no. 3, p. 513-522.
- Slattery, J.C., and Bird, R.B., 1958, Calculation of the diffusion coefficient of dilute gases and of the self-diffusion coefficient of dense gases: *American Institute Chemical Engineers Journal*, v. 42, p. 137-142.
- van Genuchten, M.Th., 1980, A closed-form equation for predicting the hydraulic conductivity of unsaturated soils: *Soil Science Society of America Journal*, v. 44, p. 892-898.
- Warner, M.J., and R.F. Weiss, 1985, Solubilities of chlorofluorocarbons 11 and 12 in water and seawater, *Deep-Sea Research*, v. 32, p. 1485-1497.